

# Radiation dose and image quality evaluation relative to different contrast media using cone-beam CT

**Aims:** To evaluate the radiation dose and image quality of an adult cone-beam CT (CBCT) with oil-based (OBC) and water-soluble contrast (WSC) material. **Materials & Methods:** A total of 44 patients, range: 46–82 years, (male:female–26:18) who underwent CBCT examination during transarterial chemoembolization. Each patient received two CBCT scans; energy used:  $94.4 \pm 4.75$  kV (mean  $\pm$  standard deviation), current:  $424 \pm 132$  mA for WSC and  $94.5 \pm 4.7$  kV,  $423.5 \pm 132$  mA for OBC. The volume of WSC material injected was 12 ml and OBC was 4 ml. **Results:** WSC examination showed significantly ( $p < 0.05$ ) decreased (5.83%) dose–area product compared with OBC. Hounsfield unit, noise, signal–noise ratio and contrast–noise ratio was higher for OBC (49.4, 19.44, 38 and 58%, respectively) compared with WSC ( $p < 0.05$ ). Qualitative assessment of WSC data (median: 2, interquartile range: 1.5–2.5) showed higher image quality compared with OBC data (2.7, interquartile range: 2.3–3.9). **Conclusion:** A detectable reduction of radiation dose was achieved with WSC compared with OBC in CBCT imaging. Quantitative image–quality parameters reflect higher values for OBC compared with WSC in the liver parenchyma. Subjective analysis showed an exactly opposite result due to the streak artifacts from OBC material.

**KEYWORDS:** cone-beam CT • image quality • oil-based contrast • radiation dose • transarterial chemoembolization • water-soluble contrast

Advances in imaging parameters have made it possible to obtain 3D CT-like slices from multiple digital subtraction angiography images placed at various projection angles and rotated around a patient [1]. Cone-beam CT (CBCT) is an advanced imaging system that uses a flat panel detector to acquire and display images in a 3D format [2]. The technique of CBCT allows varying soft tissue contrast images in multiple viewing planes, which is an improvement over its counterparts, the conventional single-planar digital subtraction angiography and x-ray scanners [1,3]. It has been reported in previous studies that advances in angiographic interventions, such as transcatheter embolization and targeted intravascular oncologic procedures, have increased the need for accurate 3D characterization of organs and anatomical structures in the region of examination [2,4]. Several studies have shown the capability of CBCT of producing decreased radiation and intravenous contrast doses compared with CT angiography [5,6]. The major difference between CBCT and multidetector CT is the increase in scattered radiation, mostly present in the CBCT scanners, which occurs due to the wider x-ray beam collimation seen in the scanners and leads to a significant degradation of image quality. This problem is absent in the multidetector CT due to the presence of anti-scatter septae between the individual detector

channels [7,8]. Furthermore, beam hardening and truncated projections are other major challenges faced by CBCT image reconstruction in general [9]. Due to the increase in frequency of CBCT examination, higher radiation doses have raised concerns about patient doses and safety compared with the doses used in other conventional x-ray diagnoses.

Oil-based contrast (OBC) agents and water-soluble contrast (WSC) agents are known to have a high atomic number material (iodine atomic number = 53, K-shell binding energy = 33.2 keV), which absorbs more radiation than substances with lower atomic numbers. The presence of such material within the patient's body may change the image quality, as well as patient radiation dose. This may be due to the differences in concentration, volume and density of both OBC and WSC material injected into the patient. These concerns prompted the formulation of this study. This research attempts to evaluate the effect of OBC (lipiodol) and WSC (visipaque) material on radiation dose and image quality of an adult CBCT.

## Materials & methods

### ■ Patient selection

A total of 44 patients (26 males and 18 females; mean age:  $64.1 \pm 10.9$ , range: 46–82 years) were included in this retrospective study

Jijo Paul\*<sup>1</sup>,  
Thomas J Vogl<sup>1</sup> &  
Emmanuel C Mbalisike<sup>1</sup>

<sup>1</sup>Department of Diagnostic & Interventional Radiology, JW Goethe University Hospital Frankfurt/Main, Theodor-Stern-Kai 7, 60590 Frankfurt/Main, Germany

\*Author for correspondence:  
Tel.: +49 173 962 7031  
Fax: +49 696 301 7258  
jijopaul1980@gmail.com

Future  
Medicine  part of 

who received transarterial chemoembolization (TACE) treatment between March 2010 and October 2011. Institutional review board approval was obtained for this retrospective data analysis. All patients receiving TACE for at least a single hepatic lesion were included in this study. The exclusion criteria for TACE were patients who could not withstand TACE, that is, patients who had various contraindications to the therapy, such as extra-hepatic tumors, poor performance status, poor liver function, cardiovascular or respiratory failure, obstructive jaundice, renal compromise or failure, florid infections, infection around the femoral region and contraindication to angiography. Further patients excluded from this study were those who were receiving radiation therapy treatment or had been exposed to radiation in the previous month.

#### ■ CBCT examination

The CBCT examinations were performed using a floor-mounted robotic flat panel angiography system (Artis Zeego multiaxis system, Siemens Healthcare, Germany) (FIGURE 1). Every patient received two CBCT scans; the first scan was performed during the time of WSC injection into the hepatic artery. The second scan was 2–3 min after the injection of OBC into the targeted hepatic artery. This time interval was necessary so that the interventionist and his assisting radiologist could assess the WSC image data set before the OBC material was injected. Each CBCT scan was accomplished with a double rotation (rotation one and two) of the x-ray source and detector system around the patient (standard scan technique recommended by manufacturer). The scan parameters used for this study are mentioned in TABLE 1. The exposure time taken for each rotation was 5 s, for a total of 10 s for each scan, and the automatic



**Figure 1.** Cone-beam CT (Artis Zeego) used for the study.

exposure control was utilized for all scans. The reconstruction parameters were 0.7 mm slice thickness,  $512 \times 512$  mm<sup>2</sup> matrix size, and 48 cm input field. A fixed 60 frames/s was used to acquire image data, since the number of frames affects image reconstruction. The detector system is made up of a cesium iodide scintillator embedded in a hydrogenated amorphous silicon layer. 12 ml of water-soluble iodinated contrast material (Visipaque™ 320; General Electric Healthcare, Braunschweig, Germany) was injected into the hepatic arteries at the time of the first scan. The WSC material injected was diluted with 36 ml of saline in a standard ratio of 1:3. During the injection, patients were instructed to hold their breath until the completion of the rotational run of the x-ray tube detector system, which typically required a single breath-hold of 12 s. The post-OBC (Lipiodol®; Guerbet Laboratory, Aulnay-sous-Bois, France) imaging was performed 2–3 min after 4 ml (1.96 g of iodine) of lipiodol was injected into the target hepatic artery. The raw data acquisition and 3D reconstruction were performed by the Leonardo workstation in 30–60 s. Using the CT principle, acquired raw data were utilized to reconstruct the patient's images for diagnostic purpose by Dyna CT®. The images obtained from the water-soluble and OBC material scans were later viewed and evaluated using a dedicated Radiology Information Systems/Picture Archiving and Communications Systems workstation (Centricity 4.1, General Electric Healthcare, Dornstadt, Germany) [10].

#### ■ Image & data analysis

Imaging of the upper abdominal region was performed using a CBCT to include the full liver in the scan field of view. Two independent radiologists specialized in medical imaging evaluations of the WSC and OBC image data sets. Both investigators have more than 6 years of experience following their doctorate degrees in diagnostic radiology. The image data sets obtained for both the WSC and OBC were viewed in a multiplanar format with the X-Leonardo workstation (Siemens Healthcare). All images were evaluated using the PACS system and image analyses were performed in consensus by the two investigators. The two investigators had previously agreed on four specific anatomical locations for regions of interest measurements, which they later evaluated separately on their own. A region of interest (done by drawing a circle) of 2 cm in diameter was chosen in the

Table 1. Details of the scan parameters and patient characteristics used.

Patient/scan parameters	WSC, mean $\pm$ SD (range)	OBC, mean $\pm$ SD (range)
Age (years)	64 $\pm$ 11 (56–73)	64 $\pm$ 11 (56–73)
Gender (male:female)	26:18	26:18
Patient internal diameter (mm)	162.7 $\pm$ 21 (143–197)	162.8 $\pm$ 21 (142–196)
Contrast material (ml)	12.0 (3.84 g iodine)	4 (1.96 g iodine)
Field size (cm)	30 $\times$ 38	30 $\times$ 38
Scan start position	0°	
Scan end position	300°	
Speed of rotation	60°/s	

OBC: Oil-based contrast; SD: Standard deviation; WSC: Water-soluble contrast.

parenchymatous part of the liver, away from the lesion, in four different slices, so that values for the Hounsfield unit (HU liver) and the image noise (standard deviation) could be obtained. The investigators then agreed on the averages that would be used to derive the statistics. Signal-to-noise ratio (SNR) was determined by HU liver/image noise. In addition, HU data of soft tissue muscle (HU muscle) was collected and these were used to determine the contrast-to-noise ratio (CNR = [HUliver-HUmuscle]/image noise [liver]) [11].

Qualitative analyses were performed by both investigators and an additional medical physicist (with 7 years experience), and they were completely blinded from the scan parameters. The investigators were allowed to adjust the window level and window width independently, according to their own interest, to view images appropriately, and it represented the actual clinical condition for both image data sets during the assessment. The assessment was purely based on a five point scale:

- One: excellent visual image quality delineation of lesion;
- Two: good quality image and the possibility of differentiating lesions and vessels;
- Three: moderate differentiation of vessels and lesion;
- Four: image reading is still possible but significantly reduced confidence levels;
- Five: poor image quality and images not used for diagnostic purpose.

#### ■ Dose calculation

Dose–area product (DAP) is a parameter used for the evaluation of radiation risk from diagnostic x-ray examination and interventional procedures. It considers the dose within the radiation field, as well as the area of tissue

irradiated. Therefore, DAP may be a better indicator of the overall risk of inducing cancer than the dose within the field. DAP is a physical dose parameter that cannot be used for the radiation risk evaluation directly. Conversion coefficients (convert from DAP values to effective dose for certain exposure types and irradiation areas) for a specific examination protocol are needed if further evaluations are performed. Furthermore, information on organ doses is required for more appropriate radiation risk evaluation. CBCT has the advantage of the permanent installation of a DAP meter on the tube housing for easier radiation dose measurement. The radiation dose parameters were obtained from the system control console and this was used to calculate the total dose from the CBCT examination received by each patient. The dose descriptors, such as DAP and patient entrance dose, as recommended by the manufacturer, were used for the reporting of the radiation dose. The parameters, such as table height, position, field of view and collimation used for the scan of all patients, were similar so that DAP is an adequate measure of radiation dose. The table height, field of view and other machine parameters were fixed for the protocol that was used in this study for all patients. The CBCT system is integrated with a DAP meter mounted on the x-ray source housing. All dose values reported here are collected from the patient protocol description obtained from the examination unit. The total DAP, in Gy $\text{cm}^2$ , was calculated from the output of the dose measuring device (DAP meter). Patient entrance dose (skin entrance dose) in mGy was calculated with respect to the reference conditions published by the International Electrotechnical Commission standard 60601-2-43 [12].

#### ■ Statistical analysis

Statistical analyses were performed using dedicated statistical software BiAS 9.02 (Epsilon

Verlag, Frankfurt, Germany). The *p*-value of equal to or less than 0.05 was considered to be statistically significant. Continuous variables were treated as mean  $\pm$  standard deviation and range. The Shapiro–Wilk test was used to assess the normality of data distribution. The patient internal abdominal diameter and quantitative image analysis (including signal intensity in HU, image noise, SNR and CNR) were tested between the two groups. An appropriate statistical test used to determine the level of significance was the two-sided student's *t*-test. A similar test was used to determine the significance of the two groups for tube current and energy. For the qualitative image analysis, the paired *t*-test was used to compare the subjective image quality of the both data sets.

## Results

### ■ Patient features

All CBCT examinations performed in this study were used to monitor the TACE procedure and were successfully completed without any complications. Patient features, including thoracic inner diameter, did not differ between the two groups ( $p > 0.05$ ) (TABLE 1).

### ■ Applied tube voltage & tube current

Mean kV-values were lower in WSC ( $94.3 \pm 4.7$  and  $94.5 \pm 4.8$ ) compared with OBC ( $94.4 \pm 4.6$  and  $94.6 \pm 4.8$ ) and were statistically nonsignificant to each other (all  $p > 0.05$ ) (TABLE 2). Mean tube current was lower in rotation one (WSC:  $422 \pm 132$ , OBC:  $422 \pm 132$ ) compared with rotation two (WSC:  $426 \pm 138$ , OBC:  $425 \pm 132$ ) and was statistically significant ( $p < 0.0001$ ). However, the intercomparison between WSC and OBC showed no significant difference ( $p = 0.966$ ,  $p = 0.9172$ , respectively).

### ■ Radiation dose

The normality of the distribution of the DAP values and patient entrance doses analyzed showed a *p*-value of  $>0.1$ . Mean DAP values were lower in WSC (rotation one:  $29.2 \pm 8$  Gy $\text{cm}^2$ , rotation two:  $29.22 \pm 8$  Gy $\text{cm}^2$ ) compared with OBC (rotation one:  $31 \pm 7.8$  Gy $\text{cm}^2$ , rotation two:  $31.1 \pm 7.8$  Gy $\text{cm}^2$ ) and yielded a statistically significant difference (*p*-values, rotation one: 0.02438, rotation two: 0.02259) (TABLE 2). The DAP value showed a 5.83% deviation between groups. However, the differences of the mean DAP values were insignificant in both WSC ( $p = 0.05102$ ) and OBC ( $p = 0.0549$ ). Mean patient-entrance dose was significantly lower in WSC (rotation one:  $111.8 \pm 12.8$  mGy, rotation

two:  $111.7 \pm 13.4$  mGy) compared with OBC (rotation one:  $116.7 \pm 16$  mGy, rotation two:  $116.8 \pm 14.6$  mGy) and yielded statistical significance (rotation one: 0.02415, rotation two: 0.01892). Mean patient-entrance dose showed 4.2 and 4.4% deviation in WSC and OBC. The data are summarized in TABLE 2 and FIGURE 2, respectively. An absolute mean dose reduction (4.3%) was yielded in WSC compared with OBC.

### ■ Image quality

Mean HU was significantly lower in WSC ( $40 \pm 19$  HU) compared with OBC ( $79 \pm 24$  HU) and yielded statistical significance ( $p < 0.00001$ ; 49.4%). Mean image noise was significantly higher (19.4%) in OBC ( $72 \pm 18$  HU) compared with WSC ( $58 \pm 12$  HU). The normal distribution of both SNR and CNR data calculated showed  $p > 0.1$ , respectively. Mean SNR and CNR were higher in OBC ( $1.1 \pm 0.5$ , and  $0.6 \pm 0.4$  HU) compared with WSC ( $0.7 \pm 0.3$ , and  $0.2 \pm 0.1$  HU) (FIGURE 3); furthermore, the comparison yielded significant difference ( $p = 0.000012$  and  $p = 0.00416$ ) (TABLE 2).

In the qualitative assessment, the three observers individually graded both data sets according to a five-point score, and were expressed as a median 2 (interquartile range [IQR]: 1.5–2.5) for WSC, and 2.7 (IQR: 2.1–3.2) for OBC from observer one. For WSC median 2 (IQR: 1.6–2.6) and OBC median 2.7 (IQR: 2.2–3.2) from observer two; furthermore, 1.9 (IQR: 1.4–2.4) and 2.7 (IQR: 2.1–3.2) from observer three. The global mean score from all observers were averaged and WSC (median 2, IQR: 1.5–2.5) showed higher image quality compared with OBC (2.7, IQR: 2.3–3.9) (FIGURES 4 & 5). The comparison between the WSC and OBC data sets was significant for all observers (all  $p = 0.0001$ ); however, the interobserver comparison for WSC and OBC was insignificant ( $p > 0.05$ ).

## Discussion

The CBCT, initially introduced in the late 1990s, shows an advantage over other conventional x-ray radiograph techniques due to its increase in 3D volumetric information; however, plain x-ray radiography has a generally lower radiation dose compared with CBCT. During data acquisition with CBCT, the x-ray tube is said to orbit around the patient's body; the rotation of the C-arm is greater than  $180^\circ$  [13]. The awareness of radiation exposure is currently increasing and ways to reduce these doses are being attempted. Many clinical advantages have already been reported using the CBCT system [14–17]. The

Table 2. Quantitative assessment of the image quality and radiation dose parameters in the subgroups.

S/N	Dose/quality parameters	Water-soluble contrast (C)		Oil-based contrast (L)		p-value
		R1	R2	R1	R2	
1	Tube potential (kV)	94.3 ± 4.7 (91–101)	94.5 ± 4.8 (91–101)	94.4 ± 4.6 (91–101)	94.6 ± 4.8 (91–101)	CR1 vs CR2: 0.073 LR1 vs LR2: 0.437 CR1 vs LR1: 0.83 CR2 vs LR2: 0.853
2	Tube current (mA)	422 ± 132 (375–480)	426 ± 138 (377–491)	422 ± 132 (375–481)	425 ± 132 (377–490)	CR1 vs CR2: 0.0001 LR1 vs LR2: 0.0001 CR1 vs LR1: 0.966 CR2 vs LR2: 0.9172
3	Dose–area–product (Gycm <sup>2</sup> )	29.2 ± 8 (21–36)	29.22 ± 8 (21–38)	31 ± 7.8 (23–41)	31.1 ± 7.8 (23–40)	CR1 vs CR2: 0.05102 LR1 vs LR2: 0.0549 CR1 vs LR1: 0.02438 CR2 vs LR2: 0.02259
4	Patient entrance dose (mGy)	111.8 ± 12.8 (101–128)	111.7 ± 13.4 (101–130)	116.7 ± 16 (104–129)	116.8 ± 14.6 (105–130)	CR1 vs CR2: 0.46012 LR1 vs LR2: 0.08302 CR1 vs LR1: 0.02415 CR2 vs LR2: 0.01892
5	CT number (HU liver)	40 ± 19 (22–62)		79 ± 24 (52–109)		p < 0.00001
6	Noise (HU)	58 ± 12 (28–67)		72 ± 18 (53–98)		p < 0.00001
7	Signal-to-noise ratio	0.7 ± 0.3 (0.5–0.9)		1.1 ± 0.5 (0.9–1.2)		p = 0.000012
8	CT number (HU muscle)	38 ± 7.7 (25–44)		43 ± 9 (38–56)		p = 0.000007
9	Contrast-to-noise ratio (HU)	0.24 ± 0.1 (0.12–0.43)		0.6 ± 0.4 (0.3–0.7)		p = 0.00416

Values shown as mean ± standard deviation and range. 'R' represents x-ray tube detector rotation. C: Contrast material (water soluble); HU: Hounsfield unit; L: Lipiodol (oil based); S/N: Serial number.

current generation CBCT has to perform two rotations of the x-ray source–detector system with a speed of 60°/s (total 300°) around the patient during image data acquisition. This is not a requirement of all CBCT units; however, our system required two rotations for the image data acquisition (manufacturer specific requirement). In this study, the tube potential (energy) showed minimal absolute differences between the two x-ray exposures but there was no statistical significance. The tube current showed a difference between both rotations; however, the absolute values indicated a minimal difference. Previous studies have been done on radiation dose, image quality and scatter radiation of the CBCT [1,18,19], though few studies have attempted to show the radiation dose delivered to patients as a result of contrast materials (either WSC or OBC) injected into the patients during the examination [14,15,20,21].

Most current generation CT scanners utilize an AEC system that effectively aids the reduction of patients radiation dose and/or maintains image quality at a stable level [22]. Paul *et al.* hypothesized that the presence of iodinated contrast material leads to an increase in

radiation dose for chest examinations in CT [22]. In this study, we used a CBCT unlike that of Paul *et al.* where they used the three generations of multidetector CT. The patient entrance dose associated with OBC material was significantly higher compared with WSC and a percentage deviation of 4.3% was obtained after the comparison of both images. The DAP values showed a higher radiation dose associated with OBC compared with WSC and obtained 5.8% deviation. If the image is not bright enough, the AEC acts automatically, applying a higher radiation to the patient to generate more signal. However, an increase in radiation dose of approximately 5% obtained in this work may not be significant for TACE. The difference in radiation dose is always an important concern in the radiotherapy and radiology community, as per the 'as low as reasonably achievable' (ALARA) principle. The percentage increase in dose signifies that care must be taken with the selection, volume, concentration and type of contrast material used for the diagnostic imaging. The change in radiation dose can be explained, as the OBC material is catabolized by the liver and is cleared from liver over a period of just a few days [23].

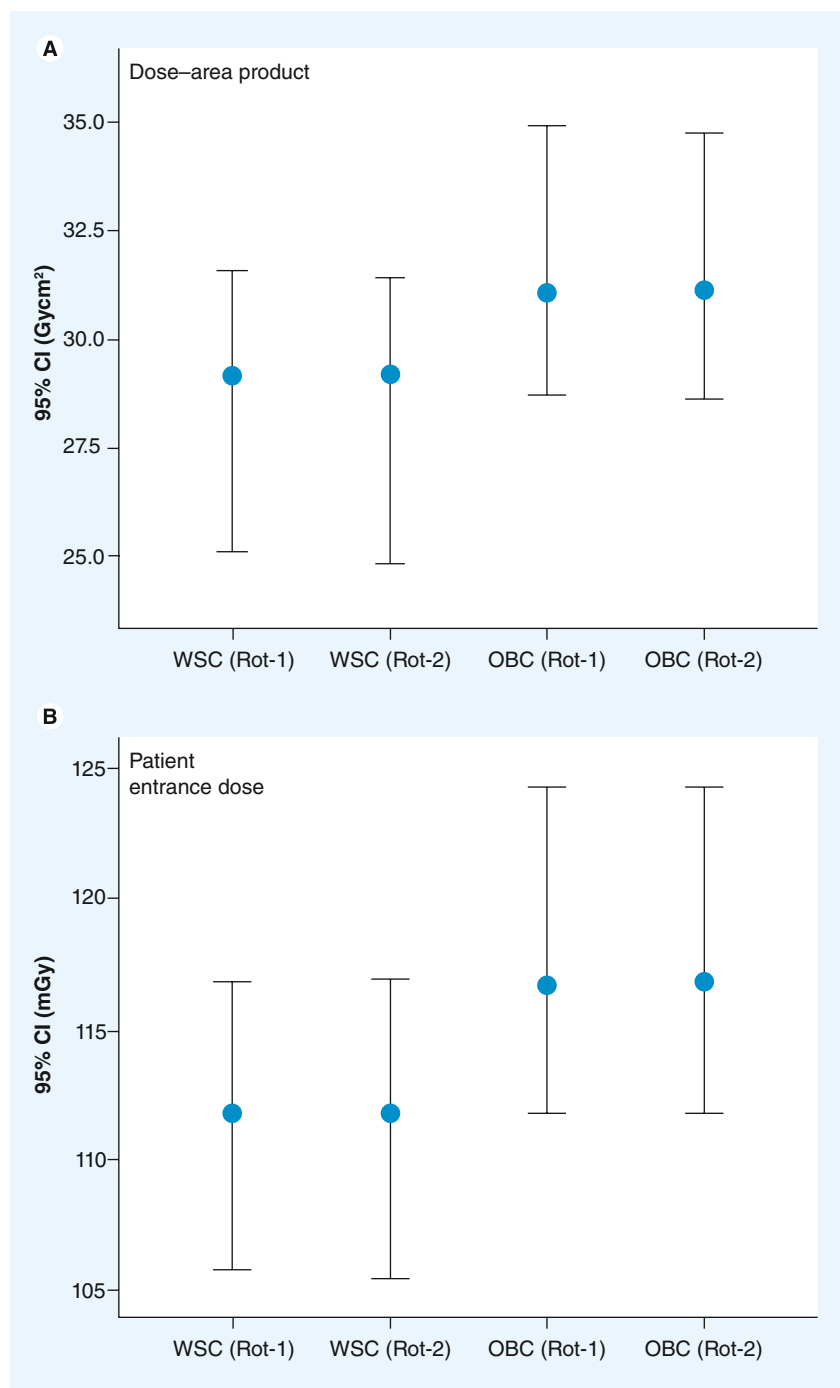


**Figure 2. Radiation dose.** Error bar shows the comparison of the radiation dose parameters, **(A)** dose–area–product (Gycm<sup>2</sup>) and **(B)** patient entrance dose (mGy), derived for different tube rotations using WSC and OBC material. OBC: Oil-based contrast; Rot: Rotation; WSC: Water-soluble contrast.

Studies are still unsure about the mechanism of stagnation of lipiodol in the hepatic parenchyma but Kabayashi *et al.* suggested that the stagnation of OBC material droplets in vessels is due to electrostatic adsorption induced by changes in the electrical charge of the inner wall [24]. This stagnation leads to an increased concentration of the OBC material in the liver

parenchyma. The process of stagnation known to occur in OBC does not exist with WSC material due to the diffusion of the contrast material through the liver parenchyma (semipermeable membrane) and filtration through the kidneys within a short period of time [25]. The stagnation process and long stay of OBC material in the region of examination leads to an increase in radiation dose for CBCT examination of upper abdominal region. As regards to the WSC material, there is a reduction of radiation dose as a result of the continual movement of injected contrast material in and out of the region of interest scanned. This is due to the presence of contrast material within the catheter (outside the exposure region) and excreted contrast material from liver to venous system.

The image quality parameters (HU, noise, SNR or CNR) are directly related to the exposure factors such as kVp and mA [26]. In this study, we observed an increase of HU in OBC data compared with the WSC data set generated using similar energy, this was due to the presence of stagnant lipiodol in the liver parenchyma (FIGURE 5). From this study, we know that the presence of accumulated OBC material in the liver and muscle enhancement due to the WSC material during OBC imaging automatically increases the HU values.

The modern CBCT scanners are equipped with an AEC, which regulates the exposure settings of the x-ray tube in order to control the attenuation of the object in the scan region. The basic principle of the AEC is to maintain the image quality for different data sets at a similar level by adjusting radiation dose.

A higher SNR and CNR were calculated using OBC images compared with WSC data because of the total amount of injected contrast material present in the liver during the examination. However, in the WSC examination, the concentration of the contrast material in the liver reduces over time. The reduction of the WSC material in the liver over time leads to a decrease in image quality. From our results, we suggest that it is necessary to further improve the performance of AEC employed in CBCT, as this helps to increase image quality. Furthermore, qualitative assessment of image quality showed that the WSC images achieved a higher image quality compared with OBC data sets. The lower image quality of the OBC image data set is due to the presence of the total amount of OBC material in the liver during the scan, which attenuates more radiation compared with WSC and produces artifacts. The

OBC material present in the liver attenuates more radiation than normal tissue because of the high atomic number, high density and high concentration that produce streak artifacts, which degrade subjective image quality, as well as increase radiation dose. When an x-ray beam passes through a patient, the lower energy photons are absorbed easily, compared with higher energy photons absorbed by the contrast material and this increases the mean energy of the x-ray beam. In other words, the detector wants to 'see' a certain amount of light and turns up the power in the presence of contrast material if it does not see enough. Applying this to OBC image data acquisition, lipiodol attenuates much radiation causing quite a few shadows to appear as beam hardening as well as streak artifacts. A relevance of comparing the OBC and WSC was to take into consideration the changes in radiation dose by using high-density materials for imaging.

Regarding the radiation dose, we agree that ALARA is of importance but we want to point out that from our study, image quality was altered by OBC material. We think, however, that increasing the speed of rotation, use of high quality detector system, AEC system and possibly reducing the volume of contrast material used can go a long way in reducing the dose the patients receive.

There have been a few limitations encountered in this study. First, we used only one CBCT scanner for all examinations. It may be beneficial to compare these data with a number of CBCT units or CBCT from different vendors. Secondly, the voluntary or involuntary motions of the patient or their internal organs (gastrointestinal tract motility) may affect the image quality or radiation dose during the time of the study. Normally, these variations are impossible to take into consideration for the assessments; we collected ample sample data to minimize these statistical errors. Finally, our research only considered the upper abdominal region and failed to take other anatomical regions into account, such as the head and neck or lower abdominal region.

### Conclusion

WSC imaging leads to a decreased DAP-value of 5.8% in comparison with OBC in a CBCT-TACE examination. The increase in dose (approximately 5%) during imaging with OBC for the treatment of the liver tumors at the time of TACE may not necessarily be regarded as a high radiation dose. However, the change in dose is a fact with respect to the contrast material

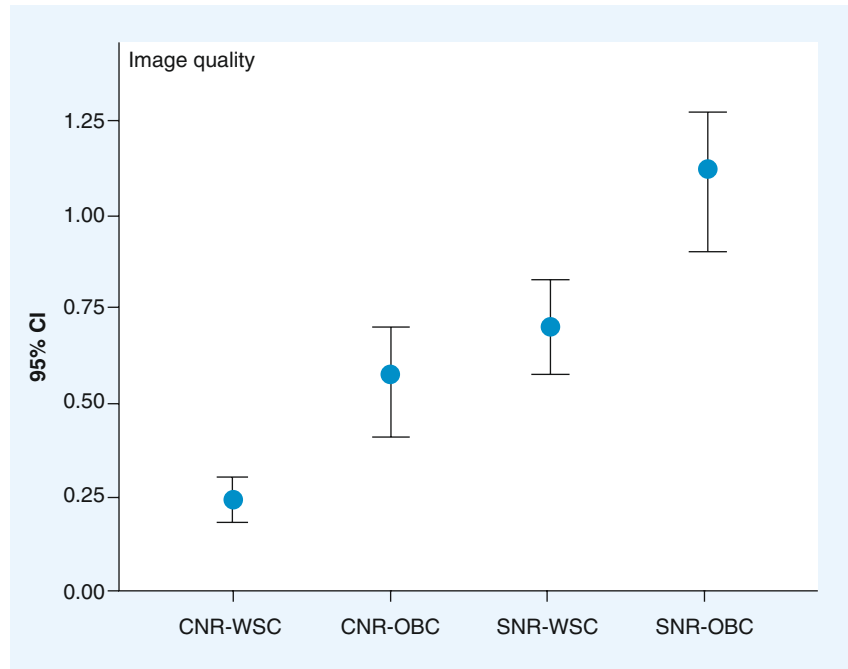


**Figure 3. Image quality.** Error bar shows the comparison of the image quality parameters (SNR and CNR) calculated from WSC and OBC data sets. A higher image quality yielded in the OBC image data set compared with WSC. CNR: Contrast-to-noise ratio; OBC: Oil-based contrast; SNR: Signal-to-noise ratio; WSC: Water-soluble contrast.

type, concentration and injection volume used for the imaging. These parameters directly affect the image quality, as well as dose, in a substantial manner and the use of OBC material for imaging should be clinically justified. Based on the image quality measurements, the HU (liver), noise, SNR, and CNR showed higher values for

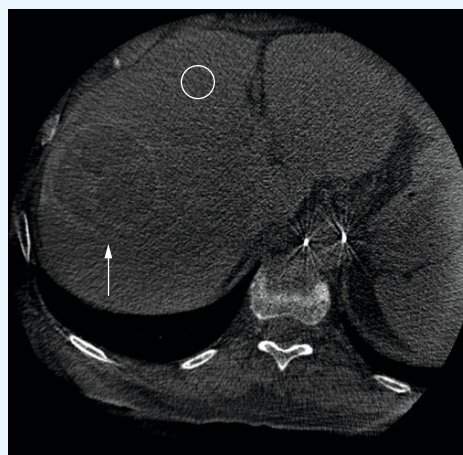


**Figure 4. Water-soluble contrast cone-beam CT image of a 60-year-old patient who presented for transarterial chemoembolization.** The white circle shows the region of interest used to measure the noise, the Hounsfield unit, and the white arrow shows the lesion present in the liver.



**Figure 5. Oil-based contrast cone-beam CT image of the same 60-year-old patient.** The white circle shows the region of interest used to measure the noise, the Hounsfield unit, and the white arrow shows the same lesion that is present in the liver in FIGURE 4.

OBC images (49.4, 19.44, 38 and 58%) compared with WSC in liver parenchyma and yielded significance. Our results suggest that further improvements need to be carried out for the AEC system of the CBCT to make image quality comparable for different image data sets including contrast studies. Subjective analysis showed exactly the opposite result due to the presence of streak artifacts arising from OBC material. The appearance of streak artifacts is due to the higher attenuation of radiation by OBC material, this leads to a decrease in subjective image quality and an increase in radiation dose.

### Future perspective

CBCT scanners can currently acquire body cross-sectional images but soft tissue image quality with different contrast materials and radiation dose has been a problem. This problem can be minimized by introduction of newer versions of CBCT scanners in the future, that is, high performance, newer reconstruction algorithms, increasing the speed and angle of rotation, the use of high quality detector systems, use of high performance electronic systems and improvement of the AEC system. These parameters could help reduce the volume of contrast material used during examination.

### Financial & competing interests disclosure

*The authors have no relevant affiliations or financial involvement with any organization or entity with a financial interest in or financial conflict with the subject matter or materials discussed in the manuscript. This includes employment, consultancies, honoraria, stock ownership or options, expert testimony, grants or patents received or pending, or royalties.*

*No writing assistance was utilized in the production of this manuscript.*

### Ethical conduct of research

*The authors state that they have obtained appropriate institutional review board approval or have followed the principles outlined in the Declaration of Helsinki for all human or animal experimental investigations. In addition, for investigations involving human subjects, informed consent has been obtained from the participants involved.*

### Executive summary

#### Radiation dose

- The dose–area product was higher (approximately 5.8%) in oil-based contrast (OBC) data compared with the water-soluble contrast data set in the cone-beam CT transarterial chemoembolization procedure. Thus, the use of OBC material for imaging should be clinically justified and caution should be taken with the type, concentration, volume of contrast used for imaging.

#### Image quality

- The comparison between OBC and water-soluble contrast data sets showed a higher image quality for OBC data sets in quantitative analysis; however, subjective analysis showed exactly the opposite result due to the presence of image artifacts.

#### Suggestion

- To maintain image quality comparable for different image data sets, including contrast studies, further improvements are required for automatic exposure control system of the cone-beam CT.

### References

- Orth RC, Wallace MJ, Kuo MD. C-arm cone-beam CT: general principles and technical considerations for use in interventional radiology. *J. Vasc. Interv. Radiol.* 19, 814–821 (2008).
- Wallace MJ, Kuo MD, Glaiberman C, Binkert CA, Orth RC, Soulez G. Three-dimensional C-arm cone-beam CT: applications in the interventional suite. *J. Vasc. Interv. Radiol.* 19, 799–813 (2008).
- Hirai T, Korogi Y, Suginozono K *et al.* Clinical usefulness of unsubtracted 3D digital angiography compared with rotational digital angiography in the pretreatment evaluation of intracranial aneurysms. *AJNR Am. J. Neuroradiol.* 24, 1067–1074 (2003).
- Iwazawa J, Ohue S, Abe H, Mitani T. Visualization of gastric varices using angiographic C-arm CT during retrograde transvenous sclerotherapy. *Indian J. Radiol. Imaging* 20(1), 39–41 (2010).
- Baba R, Konno Y, Ueda K, Ikeda S. Comparison of flat-panel detector and image-intensifier detector for conebeam CT. *Comput. Med. Imaging Graph.* 26, 153–158 (2002).
- Ishikura R, Ando K, Nagami Y *et al.* Evaluation of vascular supply with cone-beam

- computed tomography during intraarterial chemotherapy for a skull base tumor. *Radiat. Med.* 24, 384–387 (2006).
- 7 Siewerdsen JH, Jaffray DA. Cone-beam computed tomography with a flat-panel imager: magnitude and effects of x-ray scatter. *Med. Phys.* 28, 220–231 (2001).
  - 8 Endo M, Mori S, Tsunoo T, Miyazaki H. Magnitude and effects of x-ray scatter in a 256-slice CT scanner. *Med. Phys.* 33, 3359–3368 (2006).
  - 9 Schomberg H, Haar P, Baaten W. Cone beam CT using a C-arm system as front end and a spherical spiral as source trajectory. *Proc. SPIE* 7258 72580F-1 (2009).
  - 10 Bauer RW, Kramer S, Renker M *et al.* Dose and image quality at CT pulmonary angiography- comparison of first and second generation dual-energy CT and 64-slice CT. *Eur. Radiol.* 21, 2139–2147 (2011).
  - 11 Beeres M, Schell B, Mastragelopoulos A *et al.* High-pitch dual-source CT angiography of the whole aorta without ECG synchronisation: initial experience. *Eur. Radiol.* 22, 129–137 (2012).
  - 12 Sakamoto H, Aikawa Y, Ikegawa H, Sano Y, Araki T. Consideration of the newly standardized interventional reference point. *Nihon Hoshasen Gijutsu Gakkai Zasshi.* 60(4), 520–527 (2004).
  - 13 Barker E, Trimble K, Chan H *et al.* Intraoperative use of cone-beam computed tomography in a cadaveric ossified cochlea model. *Otolaryngol. Head Neck Surg.* 140(5), 697–702 (2009).
  - 14 Hwang HS, Chung MJ, Lee JW, Shin SW, Lee KS. C-arm cone-beam CT-guided percutaneous transthoracic lung biopsy: Usefulness in evaluation of small pulmonary nodules. *AJR Am. J. Roentgenol.* 195(6), W400–W407 (2010).
  - 15 Miyayama S, Yamashiro M, Okuda M *et al.* Detection of corona enhancement of hypervascular hepatocellular carcinoma by C-arm dual-phase cone-beam CT during hepatic arteriography. *Cardiovasc. Intervent. Radiol.* 34, 81–86 (2011).
  - 16 Dijkstra ML, Eagleton MJ, Greenberg RK, Mastracci T, Hernandez A. Intraoperative C-arm cone-beam computed tomography in fenestrated/branched aortic endografting. *J. Vasc. Surg.* 53(3), 583–590 (2011).
  - 17 Jin KN, Park CM, Goo JM *et al.* Initial experience of percutaneous transthoracic needle biopsy of lung nodules using C-arm cone-beam CT systems. *Eur. Radiol.* 20, 2108–2115 (2010).
  - 18 Cheng HCY, Wu VWC, Liu ESF, Kwong DL. Evaluation of radiation dose and image quality for the cone beam computed tomography system. *Int. J. Radiation Oncol. Biol. Phys.* 80(1), 291–300 (2011).
  - 19 Pouliot J, Bani-hashemi A, Chen J *et al.* Low-dose megavoltage cone-beam CT for radiation therapy. *Int. J. Radiation Oncol. Biol. Phys.*, 61(2), 552–560 (2005).
  - 20 Ganguly A, Yoon S, Fahrigr R. Dose and detectability for a cone-beam C-arm CT system revisited. *Med. Phys.* 37(5) 2264–2268 (2010).
  - 21 Smyth JM, Sutton DG, Houston JG. Evaluation of the quality of CT-like images obtained using a commercial flat panel detector system. *Biomed. Imaging Interv. J.* 2(4), e48 (2006)
  - 22 Paul J, Schell B, Kerl M, Maentele W, Vogl TJ, Bauer RW. Effect of contrast material on image noise and radiation dose in adult chest computed tomography using automatic exposure control: a comparative study between 16-, 64- and 128-slice CT. *Eur. J. Radiol.* 79(2), e128–e132 (2011).
  - 23 Luo TY, Hsieh BT, Wang SJ *et al.* Preparation and biodistribution of rhenium-188 ECD/Lipiodol in rats following hepatic arterial injection. *Nucl. Med. Biol.* 31 671–677 (2004).
  - 24 Kobayashi H, Inoue H, Shimada J *et al.* Intra-arterial injection of adriamycin/mitomycin C Lipiodol suspension in liver metastases. *Acta Radiol.* 28, 275–280 (1987).
  - 25 Schyma C, Hagemeyer L, Greschus S, Schild H, Madea B. Visualisation of the temporary cavity by computed tomography using contrast material. *Int. J. Legal Med.* 126(1), 37–42 (2012).
  - 26 Tawfik AM, Kerl JM, Bauer RW *et al.* Dual-energy CT of head and neck cancer, average weighting of low- and high-voltage acquisitions to improve lesion delineation and image quality – initial clinical experience. *Invest. Radiol.* 47(5), 306–311 (2012).